# In-Depth Kinetic Modeling and Chemical Analysis for the Epoxidation of Vegetable Oils in a Liquid–Liquid–Solid System

Yudong Meng, Nasreddine Kebir, Xiaoshuang Cai, Sébastien Leveneur

catalysts

MDPI

*Article*

# In-Depth Kinetic Modeling and Chemical Analysis for the Epoxidation of Vegetable Oils in a Liquid–Liquid–Solid System

**Yudong Meng [1,2], Nasreddine Kebir [2], Xiaoshuang Cai [3] and Sebastien Leveneur [1,*]**

[1] INSA Rouen, UNIROUEN, Normandie Univ, LSPC, UR4704, 76000 Rouen, France
[2] Laboratoire PBS, INSA Rouen Normandie, UNIROUEN, Normandie Université, UMR CNRS 6270 & FR 3038, Avenue de l'Université, 76801 Saint Etienne du Rouvray, France
[3] College of Food Science and Engineering, Henan University of Technology, Zhengzhou 450001, China
* Correspondence: sebastien.leveneur@insa-rouen.fr

**Abstract:** A heterogeneous catalyst for producing epoxidized vegetable oils, an important intermediate in the production of non-isocyanate polyurethanes, is essential for product separation and for decreasing the side-reaction, i.e., ring-opening reaction, via the Prileschajew method. The development of reliable kinetic models considering key variables for both phases and the mass transfer phenomena is missing in the literature. The reaction pathway for the ring-opening reaction is also under debate. Therefore, we studied the kinetics of epoxidation of cottonseed oil by perpropionic acid over the solid acid catalyst amberlite IR-120. An in-depth kinetic model was developed by using Bayesian inference. The reaction pathway for the ring opening was investigated. Propionic acid, a weak acid, allows for a decrease in the oxirane ring-opening side reaction.

**Keywords:** epoxidation; kinetic model; amberlite IR-120; liquid–liquid–solid

**Citation:** Meng, Y.; Kebir, N.; Cai, X.; Leveneur, S. In-Depth Kinetic Modeling and Chemical Analysis for the Epoxidation of Vegetable Oils in a Liquid–Liquid–Solid System. *Catalysts* **2023**, *13*, 274. https://doi.org/10.3390/catal13020274

Academic Editor: Mingjun Jia

Received: 5 January 2023
Revised: 23 January 2023
Accepted: 24 January 2023
Published: 26 January 2023



## 1. Introduction

Valorization of biomass can aid the chemical industry to use less fossil raw materials, thus increasing its sustainability. Vegetable oils in the chemical industry are mainly used for biodiesel production via transesterification [1–5]. The other promising use of valorizing vegetable oil is for producing polymers or materials [6–8]. Among these polymers, one can cite the production of polyurethanes, which has attracted increasing attention in recent years [9]. One way to produce non-isocyanate polyurethanes is via the aminolysis of carbonated vegetable oils [10,11].

One of the first steps in valorizing vegetable oils into polymers is the functionalization of these oils, and the epoxidation of the unsaturated groups is a good way to achieve this [12]. From a previous review [12], we have discussed several possible ways of vegetable oil epoxidation:

-Use of gaseous oxygen with the risk of over-combustion, but one needs a carrier molecule such as cumene [13];

-Direct use of hydrogen peroxide [14], but this technique was shown to work on fatty acid methyl ester and requires the use of a solvent, such as ethyl acetate;

-Use of in situ-generated percarboxylic acid, and produce the epoxidized vegetable oil via the Prileschajew method [15–17], which is the most common technique.

The Prileschajew method produces in situ percarboxylic acid from the perhydrolysis of carboxylic acid in the aqueous phase. Then, this percarboxylic acid, also known as an oxygen carrier, diffuses in the organic phase to epoxidize the unsaturated groups. This method works well because the solubility of hydrogen peroxide in the organic phase is low. Usually, an acid catalyst is used to accelerate the perhydrolysis reaction.

The number of articles concerning the use of the Prileschajew method for the epoxidation of vegetable oils is enormous. Research groups have focused on the development of catalysts (i.e., $Al_2O_3$, Amberlite, $CH_3ReO_3$, etc.) [18–20], the intensification of the liquid–liquid or liquid–liquid–solid epoxidation system [21–25], and the risk of thermal runaway [26,27]. Indeed, the Prileschajew method is liquid–liquid or liquid–liquid–solid in the case of a solid catalytic system, requiring vigorous mixing for mass and heat transfer. Furthermore, it is an exothermic reaction system, and the risk of thermal runaway is high [26,28,29].

The two main drawbacks of this reaction system are the oxirane ring-opening side reactions [30,31], and the risk of thermal runaway linked to the exothermic epoxidation. The produced percarboxylic acid was shown to be unstable [26,29]. The oxirane ring-opening side reactions occur due to the presence of protons, which activate the oxirane group. Thus, using a strong carboxylic acid, such as formic acid or homogeneous mineral acid, increases the side reaction of ring opening. The use of solid acid catalysts for perhydrolysis decreases the ring-opening reactions because the epoxidized vegetable oils cannot enter the catalyst pores. Additionally, using percarboxylic acid with a longer carbon chain can reduce acidity and improve the thermal stability of epoxidized products.

From the literature, formic and acetic acids are the most commonly used carboxylic acids [32]. Performic acid is very reactive but not thermally stable, while peracetic acid is more thermally stable but relatively strong. Thus, these acids can favor the ring-opening reaction. In order to circumvent the adverse effects of these two acids, the epoxidation of cottonseed oil by perpropionic acid over amberlite IR-120 was investigated in this study, since propionic acid is less acidic than acetic acid, and perpropionic acid is more stable than peracetic acid [33].

This reaction system involves several exothermic steps and mass transfer phenomena, making its kinetic modeling challenging. There are several kinetic modeling strategies for this system:

-Two-phase system [27,34–36]: mass transfer between the aqueous and organic phases is included. In this model, the mass transfer coefficient of different species must be evaluated or calculated;

-Pseudo-homogeneous system [30,37–41]: concentrations of species in each phase are considered, and the mass transfer phenomenon is assumed to be faster than the chemical reaction. In this model, there is no need to consider mass transfer coefficients;

-Homogeneous system [15,16,42–49]: the liquid–liquid system simplified into a homogeneous one.

To the best of the authors' knowledge, kinetic models considering the mass transfer between organic and aqueous phases, and the non-linear regression by considering the variables of the two liquid phases have not been developed and validated. To fill this gap, this study proposed such a kinetic model for the epoxidation of cottonseed oil by perpropionic acid over amberlite IR-120 in an isothermal batch reactor. An in-depth analytical study was carried out to unravel the ring-opening pathway. The development of a reliable kinetic model considering liquid–liquid mass transfer is essential for the development of industrial processes.

## 2. Results and Discussion

### *2.1. Analysis, NMR and FTIR Results, and GPC*

It is fundamental to determine the different species present during the epoxidation. This knowledge is vital for elaborating reaction pathways. For this, we used NMR, FTIR, and GPC analytical methods.

2.1.1. NMR Spectra

$^1$H NMR could be used to determine the molecule changes, and to confirm the reactions of the epoxidation and ring opening. As displayed in Figure 1, the corresponding signal of the carbon–carbon double bond (CH=CH) from 5.2 to 5.5 ppm disappeared with the presence of a signal of the epoxidized group at 3.00 ppm.

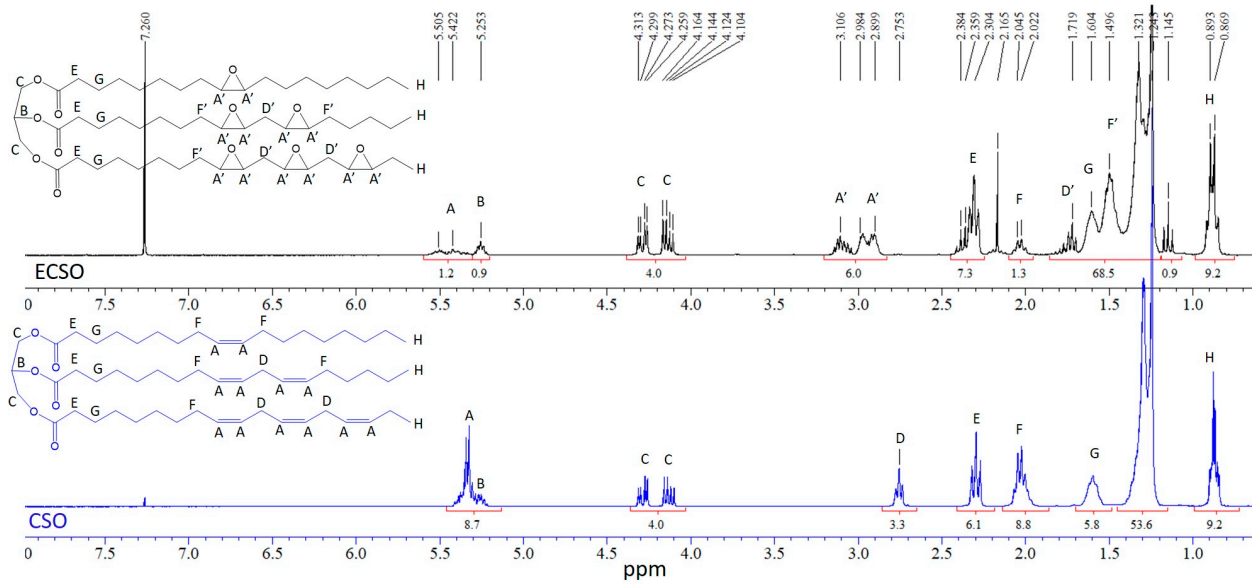


**Figure 1.** NMR spectra of CSO (cottonseed oil) and ECSO (epoxidized cottonseed oil).

The NMR spectra of intermediate samples taken during the reaction are shown in Figure 2. With the epoxidation programming, the peak intensity of the CH=CH double bond was clearly decreased, while the signal of the oxirane ring conversely appeared at 3.00 ppm.

The absence of peaks between 3.6 and 3.8 ppm in the $^1$H NMR spectra signifies the absence of hydroxyl groups resulting from hydrolytic degradation of the triglyceride, which is confirmed by the integrations of the signals of the protons in the alpha position to the oxygen of the ester groups, compared to the integration of the methyl groups. The absence of these peaks also signifies the absence of hydroxyl groups resulting from the epoxide ring opening. However, this does not mean that ring opening by water, leading to vicinal diols, did not take place, but that those elimination reactions giving access to new carbon–carbon double bonds could have taken place. This could explain the presence of a new broad peak between 5.4 and 5.6 ppm. On the other hand, the elimination reaction would also give access to enol functions, which can then be partially or totally converted into ketone functions, which are difficult to characterize from the $^1$H NMR spectra of our products.

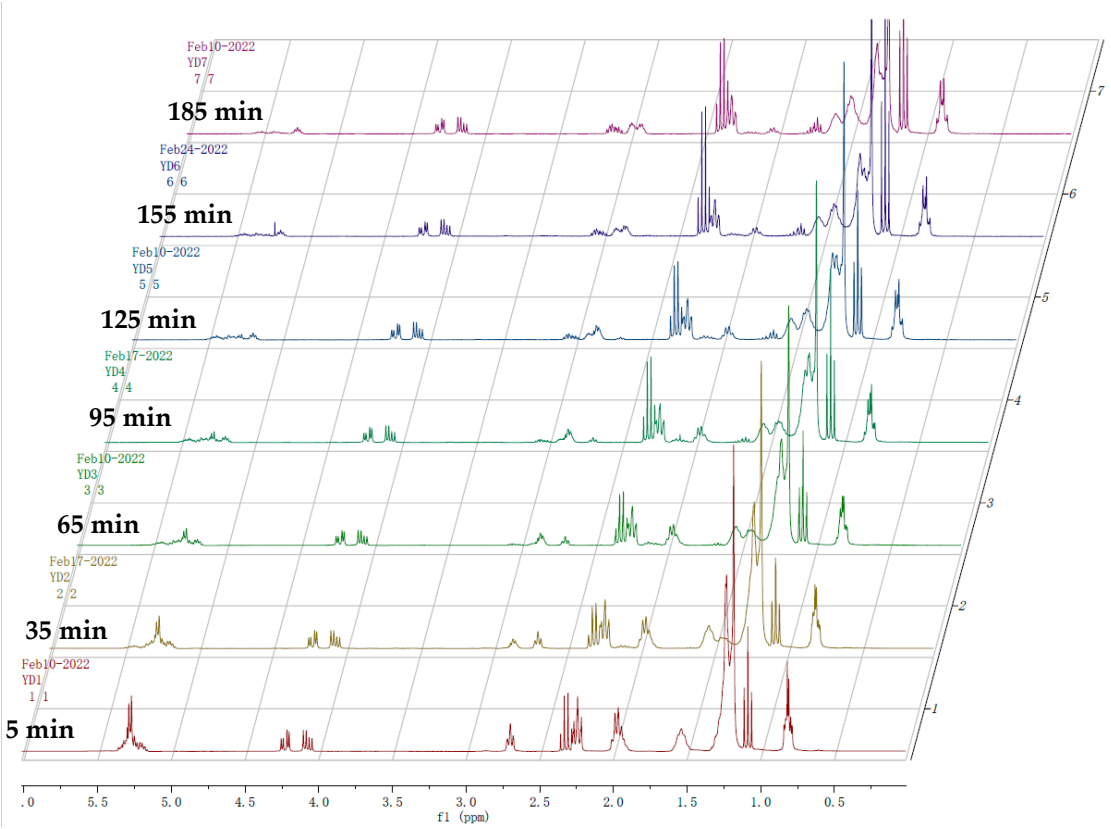


**Figure 2.** NMR spectra of CSO (cottonseed oil) and ECSO (epoxidized cottonseed oil).

2.1.2. FTIR Spectra

The FTIR spectra of CSO (cottonseed oil) and ECSO (epoxidized cottonseed oil) are displayed in Figure 3. The conversion of the CH=CH double bond in CSO as the epoxidation reaction proceeds could be verified by the disappearance of the corresponding band at about 3000-3050 $cm^{-1}$ and the presence of a band at about 850 $cm^{-1}$, corresponding to C-O-C stretching vibration of the epoxide ring in CSO.

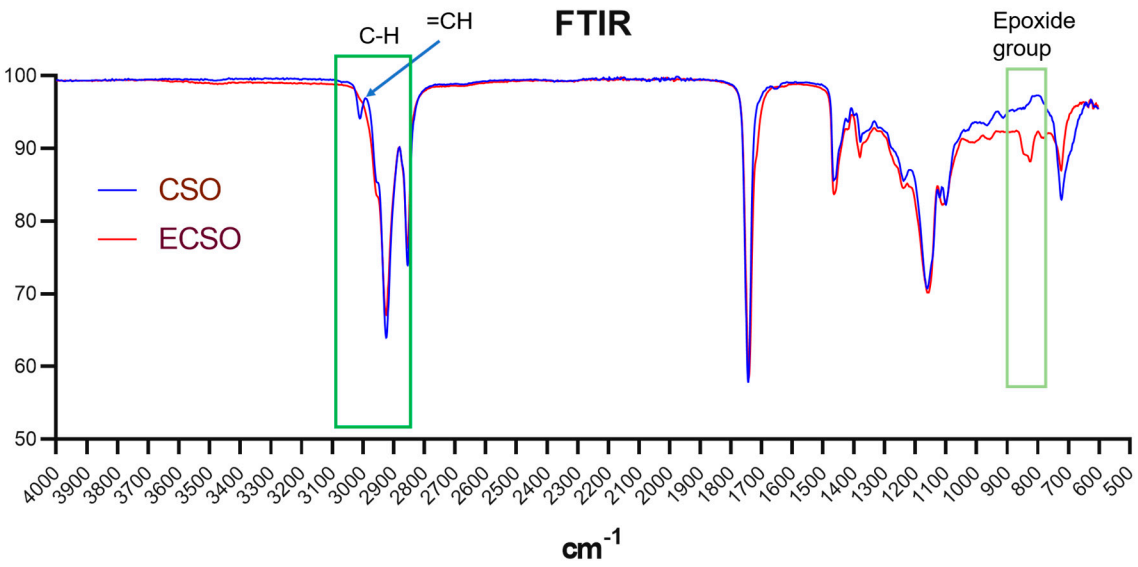


**Figure 3.** FTIR spectra of CSO (cottonseed oil) and ECSO (epoxidized cottonseed oil).

Furthermore, the intermediate samples were also monitored using FTIR (Figure 4), and the signal changes of the epoxidized group could be evidently observed with the extension of the reaction time.

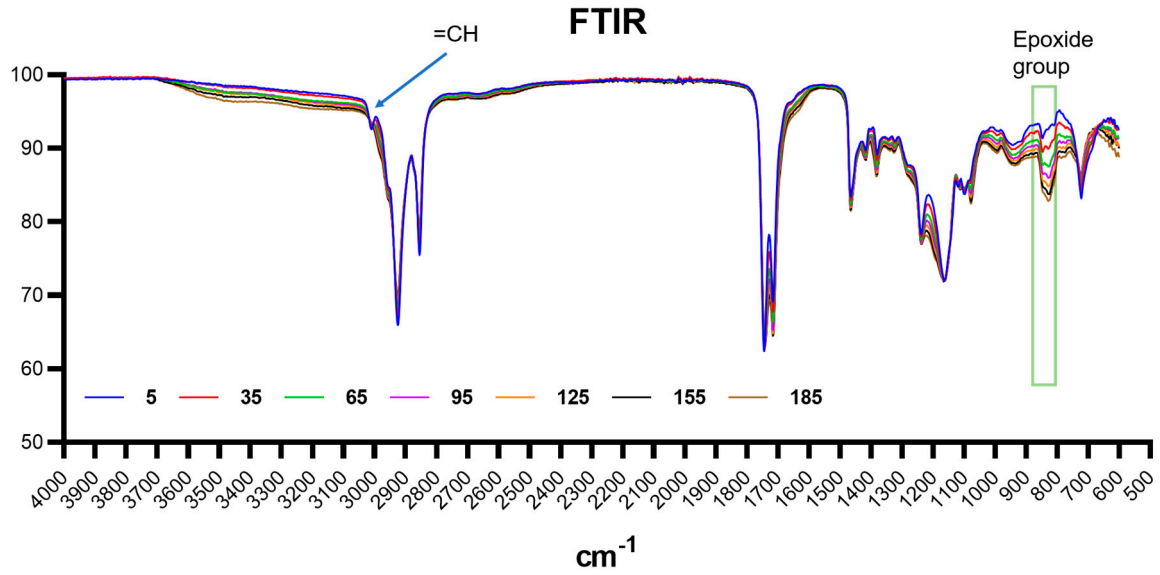


**Figure 4.** FTIR spectra of ECSO (epoxidized cottonseed oil) at different reaction times (5, 35, 65, 95, 125, 155, and 185 min) performed at 70 °C.

2.1.3. GPC

The CSO GPC chromatogram shows a narrow main peak corresponding to the triglyceride molecule (Figure 5). A very small peak of higher molecular weight can be observed, which can be attributed to a siccative minority portion of the triglyceride molecule. The ECSO GPC chromatograms show a gradual shift over time of the main peak to the higher molecular weight region, suggesting that the ring-opening products resulting from the elimination of one or two water molecules are negligible. However, the appearance of a secondary peak that increases in intensity with time suggests the presence of chain extension reactions leading to oligomers. The oligomers started to be significant after 65 min of reaction (less than 15% intensity at the end of the reaction compared to the first peak). In fact, it is well established that epoxides can undergo cationic self-polymerization in an acidic environment, leading to polyethers.

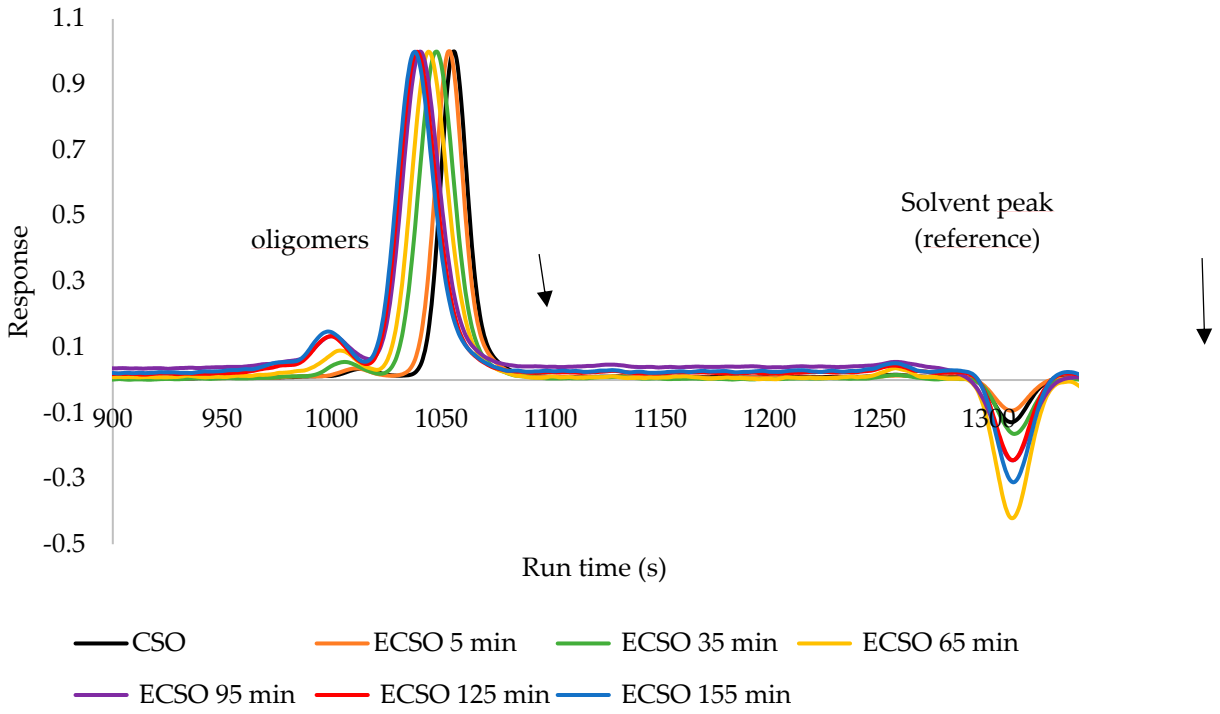


**Figure 5.** GPC chromatograms of CSO (cottonseed oil) and ECSO (epoxidized cottonseed oil) at different reaction times performed at 70 °C.

### *2.2. Effect of Reaction Temperature on the Kinetics of Epoxidation*

The effect of reaction temperature on the rate of epoxidation was observed by comparing Runs 1, 2, and 3 (Figure 6). One can notice that the rate of epoxidation increases with a reaction temperature increase from 50 °C to 70 °C. Figure 6 also shows that the ring-opening reaction occurs in conjunction with the epoxidation reaction.

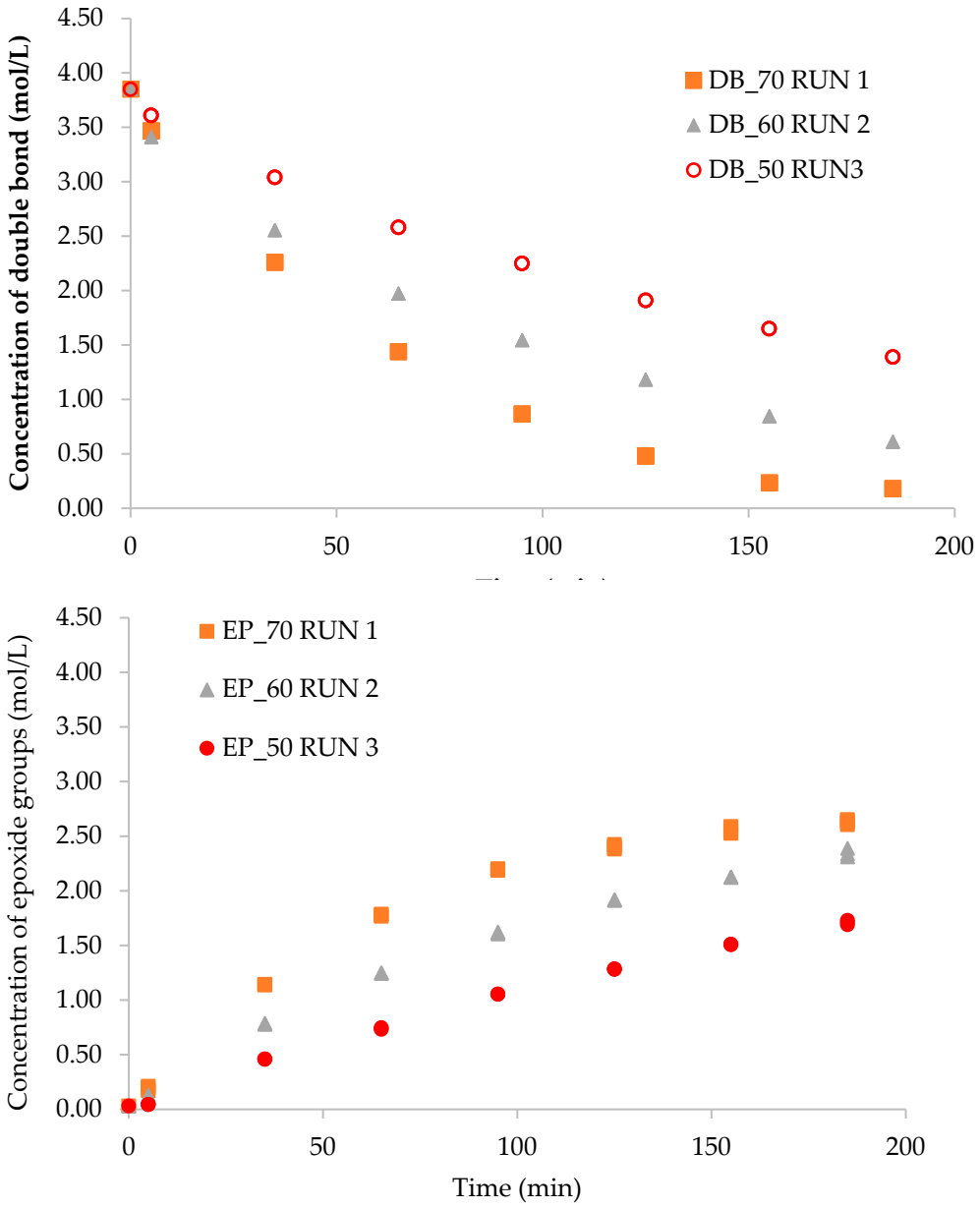


**Figure 6.** Effect of reaction temperature on the rate of epoxidation.

*2.3. Effect of HP/PA Ratio on the Kinetics of Epoxidation*

The ratio of initial concentrations of hydrogen peroxide to propionic acid ($\frac{[HP]_{0,as}}{PA_{0,as}}$) in the aqueous phase can play a role in the rate of perhydrolysis, and, thus, in the rate of epoxidation. Figure 7 shows this effect on the rate of epoxidation for Runs 2, 5, and 6. Figure 7 shows that the initial concentration ratio does not significantly impact the initial reaction rate of epoxidation, even if one can notice that an increase in $\frac{[HP]_{0,as}}{PA_{0,as}}$ has a slight tendency to increase the rate of epoxidation. The kinetic of Run 5 is slightly faster than those of Runs 2 and 6 (lowest ratio $\frac{[HP]_{0,as}}{PA_{0,as}}$). However, after 60 min of reaction, one can notice that the kinetic of Run 5 is faster, and the final concentration of epoxide groups is higher than those of Runs 2 and 6. This phenomenon could be explained by the fact that a higher amount of hydrogen peroxide ensures a faster production of perpropionic acid,

and perpropionic acid is more stable than peracetic acid [48], thus, the thermal decomposition of perpropionic acid can be negligible.

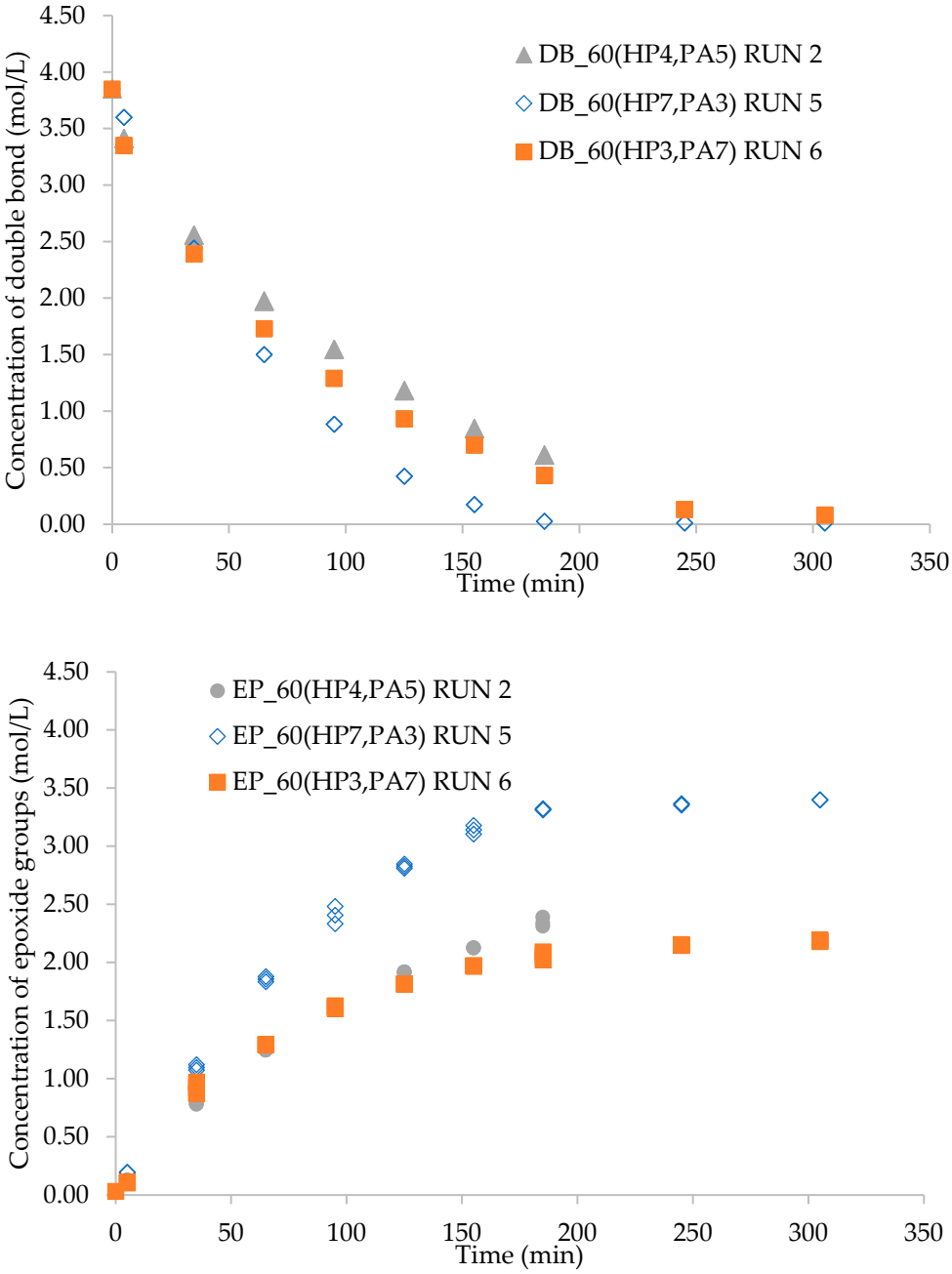


**Figure 7.** Effect of $\frac{[HP]_{0,as}}{PA_{0,as}}$ on the rate of epoxidation.

### *2.4. Catalyst Loading Effect on the Kinetics of Epoxidation*

The catalyst Amberlite IR-120 catalyzes the perhydrolysis reaction [48,50], in other words, the rate of perpropionic acid production. Runs 2 and 4 were compared to evaluate the effect of catalyst loading on the rate of epoxidation. Figure 8 shows that the rate of epoxidation increases with the increase in catalyst loading from 5 to 10 g. The presence of ring-opening reactions can be also noticed based on comparing the concentrations of DB and EP at 185 min.

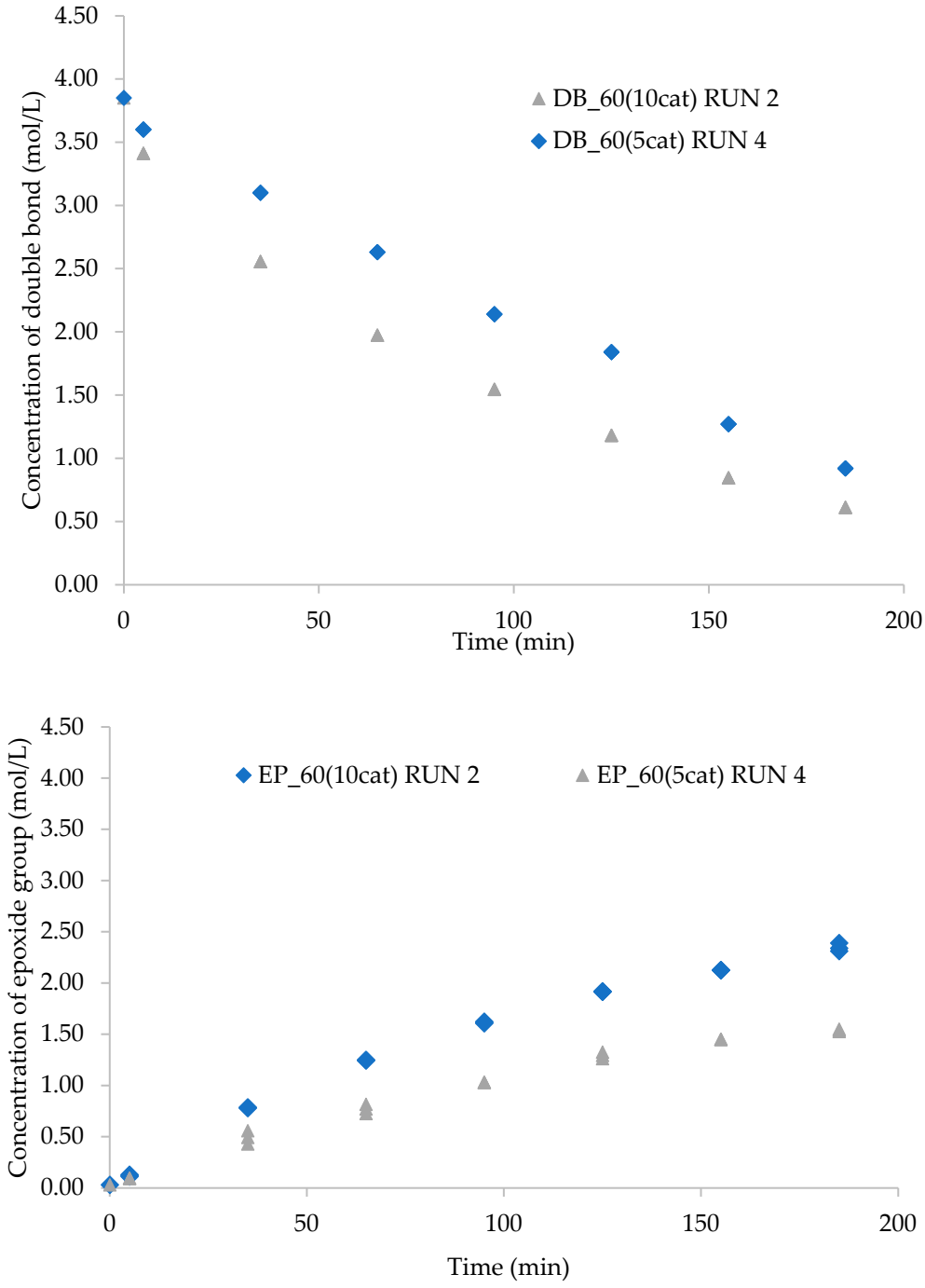


**Figure 8.** Effect of catalyst loading on the rate of epoxidation.

## 3. Kinetic Modeling

The modeling consisted of two stages: regression to estimate the kinetic constants, and validation to evaluate the reliability of the models. We used a hold-out method, i.e., 10 experiments were used for the regression stage, and two experiments were used for the validation stage [51,52]. Tables 1 and 2 show the selected experiments for both stages.

For the epoxidation experiments, we found that by fixing the rotating speed at 600 rpm, there is no effect of the rotation velocities on the kinetics.

Athena visual studio was used for the modeling [53].

**Table 1.** Experimental matrix for the modeling of epoxidation of cottonseed oil. (DB: double bond, EP: epoxide, PA: propionic acid, and HP: hydrogen peroxide).

| | | | Initial Mass (g) | | | | Initial Concentration (mol/L) | | | | |
|---|---|---|---|---|---|---|---|---|---|---|---|
| **Run** | **T (K)** | **Catalyst** | **CSO** | **33% HP** | **PA** | **$H_2O$** | **$[H_2O]_{aq}$** | **$[DB]_{org}$** | **$[Ep]_{org}$** | **$[HP]_{aq}$** | **$[PA]_{aq}$** |
| 1 | 341.05 | 10.20 | 100.10 | 85.30 | 73.00 | 42.10 | 27.51 | 3.85 | 0.03 | 4.13 | 4.92 |
| 2 | 331.84 | 9.80 | 100.10 | 84.50 | 74.00 | 44.00 | 27.60 | 3.85 | 0.03 | 4.05 | 4.93 |
| 3 | 323.15 | 10 | 100.10 | 86.30 | 73.30 | 42.90 | 27.63 | 3.85 | 0.03 | 4.14 | 4.89 |
| 4 | 333.15 | 5 | 100.00 | 83.00 | 74.00 | 43.00 | 27.39 | 3.85 | 0.03 | 4.03 | 4.99 |
| 5 | 333.15 | 10 | 100.00 | 144.60 | 44.50 | 11.00 | 29.95 | 3.85 | 0.03 | 7.01 | 3.00 |
| 6 | 333.15 | 10 | 100.00 | 61.80 | 103.71 | 34.35 | 21.06 | 3.85 | 0.00 | 3.00 | 7.00 |
| 7 | 353.15 | 5 | 100.00 | 83.00 | 74.00 | 43.00 | 27.39 | 3.85 | 0.03 | 4.03 | 4.99 |
| 8 | 323.15 | 15 | 100.10 | 86.30 | 73.30 | 42.90 | 27.63 | 3.85 | 0.03 | 4.14 | 4.89 |
| 9 | 353.15 | 2 | 100.00 | 83.00 | 74.00 | 43.00 | 27.39 | 3.85 | 0.03 | 4.03 | 4.99 |
| 10 | 343.15 | 10 | 100.00 | 83.00 | 74.00 | 43.10 | 27.63 | 3.33 | 0.53 | 4.14 | 4.89 |

**Table 2.** Experimental matrix for the validation of epoxidation of cottonseed oil model. (DB: double bond, EP: epoxide, PA: propionic acid, and HP: hydrogen peroxide).

| | | | Initial Mass (g) | | | | Initial Concentration (mol/L) | | | | |
|---|---|---|---|---|---|---|---|---|---|---|---|
| **Run** | **T (K)** | **Catalyst** | **CSO** | **33% HP** | **PA** | **$H_2O$** | **$[H_2O]_{aq}$** | **$[DB]_{org}$** | **$[Ep]_{org}$** | **$[HP]_{aq}$** | **$[PA]_{aq}$** |
| 1V | 328.15 | 4.00 | 100.04 | 103.00 | 89.00 | 8.00 | 21.39 | 3.85 | 0.03 | 5.00 | 6.01 |
| 2V | 338.15 | 8.00 | 100.04 | 103.00 | 59.00 | 38.00 | 29.73 | 3.85 | 0.03 | 5.00 | 3.98 |

### *3.1. Kinetics*

Based on the preliminary experimental studies, three main reactions are involved in the epoxidation of cottonseed oil: perhydrolysis of propionic acid, epoxidation of the unsaturated group (-CH=CH-) by perpropionic acid, and oxirane ring-opening side reaction. Figure 9 shows the different reaction steps.

The perhydrolysis step, i.e., the production of perpropionic acid, is catalyzed by the cation exchange resins. We assumed that the proton motion from the Amberlite IR-120 is free [50,54]. The solubility of hydrogen peroxide in the organic phase is low [34,37,40,41]. Thus, the perhydrolysis reaction mainly occurs in the aqueous phase.

The perhydrolysis expression rate was expressed as:

$$R_{Perh} = k_{Perh} \cdot m_{dried\ cat} \cdot \left( [PA]_{aq} \cdot [HP]_{aq} - \frac{1}{K_{eq}} \cdot [PPA]_{aq} \cdot [W]_{aq} \right) \quad (1)$$

where $K_{eq}$ is the equilibrium constant and $m_{dried\ cat}$ is the Amberlite IR-120 based on a dried basis.

The expression rate for the epoxidation was expressed as:

$$R_{Ep} = k_{Ep} \cdot [PPA]_{org} \cdot [DB]_{org} \quad (2)$$

where $[DB]_{org}$ is the concentration of the unsaturated group from the cottonseed oil.

As from a previous article of our group [40], the ring-opening reaction was derived by assuming that the rate-determining step is the protonation of the oxirane group. Thus, the rate is expressed as:

$$R_{RO} = k_{RO} \cdot [Ep]_{org} \cdot \left( \frac{[PA]_{aq}}{[W]_{aq}} \right)^{0.5} \quad (3)$$

In Equation (3), the source of protons comes from the dissociation of propionic acid in the aqueous phase. The proton transfer from the aqueous to the organic phase is supposed to be very fast [37,40]. Protons from the Amberlite IR-120 are mainly located inside

the resins [50]. Thus, one can neglect the protonation of the oxirane group by these protons for steric hindrance reasons.

To decrease the estimation number of parameters, the perhydrolysis kinetics of propionic acid were studied and modeled separately following the same procedure as described in previous articles [55,56].

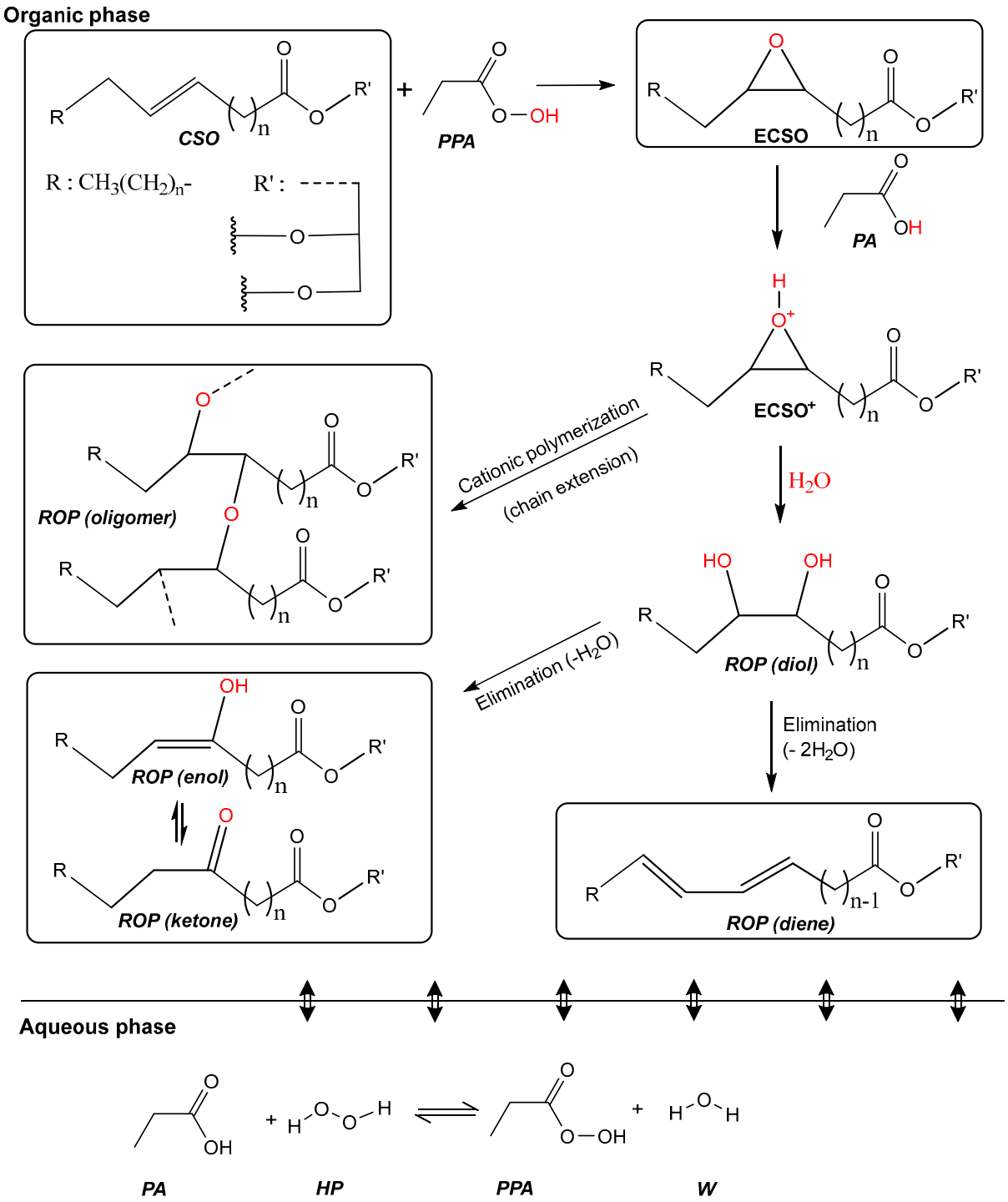


**Figure 9.** Reaction pathway for the epoxidation of cottonseed oil by perpropionic acid. (DB: double bond, EP: epoxide, ROP: ring-opening products, W: water, PPA: perpropionic acid, PA: propionic acid, and HP: hydrogen peroxide).

*3.2. Material Balances*

Due to the vigorous stirring, no macroscopic gradient was considered in this study. Furthermore, reaction temperatures were recorded to be constant during a reaction. Thus, isothermal mode was used.

The solubilities of cottonseed oil and cottonseed oil-derivatives in the aqueous phase were neglected. The solubilities of hydrogen peroxide and water in the organic phase were not considered. The aqueous phase was the continuous phase, and the catalyst was assumed to be mainly wetted by this phase during the epoxidation. Volumes of the organic and aqueous phases were assumed to be constant during the reaction.

The double-film theory was used to consider the mass transfer phenomenon, and mass transfer resistance from the aqueous phase, i.e., the continuous phase, was supposed to be negligible. Thus, the concentration of species $i$ at the aqueous interface, noted as $[i]^*_{aq}$, is the same as the concentration of species $i$ in the bulk aqueous phase, noted as $[i]_{aq}$.

The distribution coefficient or equilibrium molar ratio of a compound $i$, $K_i$, is defined as:

$$K_i = \frac{[i]^*_{aq}}{[i]^*_{org}} \tag{4}$$

where $[i]^*_{org}$ is the concentration of compound $i$ at the organic interface. The concentration $[i]^*_{org}$ can be expressed as: $[i]^*_{org} = \frac{[i]^*_{aq}}{K_i} \approx \frac{[i]_{aq}}{K_i}$.

Material balances for the different species are:

$$\frac{d[DB]_{org}}{dt} = -R_{Ep} \tag{5}$$

$$\frac{d[Ep]_{org}}{dt} = R_{Ep} - R_{RO} \tag{6}$$

$$\frac{d[RO\ products]_{org}}{dt} = R_{RO} \tag{7}$$

$$\frac{d[PA]_{org}}{dt} = R_{Ep} + \frac{k_{PA-org} \cdot a}{V_{org}} \cdot \left([PA]^*_{org} - [PA]_{org}\right) = R_{Ep} + \frac{k_{PA} \cdot a}{V_{org}} \cdot \left(\frac{[PA]_{aq}}{K_{PA}} - [PA]_{org}\right) \tag{8}$$

$$\frac{d[PPA]_{org}}{dt} = -R_{Ep} + \frac{k_{PPA-org} \cdot a}{V_{org}} \cdot \left([PPA]^*_{org} - [PPA]_{org}\right) = -R_{Ep} + \frac{k_{PPA-org} \cdot a}{V_{org}} \cdot \left(\frac{[PPA]_{aq}}{K_{PPA}} - [PPA]_{org}\right) \tag{9}$$

$$\frac{d[PA]_{aq}}{dt} = -R_{Perh} - \frac{k_{PA-org} \cdot a}{V_{org}} \cdot \left([PA]^*_{org} - [PA]_{org}\right) = -R_{Perh} - \frac{k_{PA-org} \cdot a}{V_{org}} \cdot \left(\frac{[PA]_{aq}}{K_{PA}} - [PA]_{org}\right) \tag{10}$$

$$\frac{d[PPA]_{aq}}{dt} = R_{Perh} - \frac{k_{PPA-org} \cdot a}{V_{org}} \cdot \left([PPA]^*_{org} - [PPA]_{org}\right) = R_{Perh} - \frac{k_{PPA-org} \cdot a}{V_{org}} \cdot \left(\frac{[PPA]_{aq}}{K_{PPA}} - [PPA]_{org}\right) \tag{11}$$

$$\frac{d[HP]_{aq}}{dt} = -R_{Perh} \tag{12}$$

$$\frac{d[W]_{aq}}{dt} = R_{Perh} \tag{13}$$

where $k_{PPA-org}$ and $k_{PA-org}$ are mass transfer coefficients of PA and PPA in the organic phase, $a$ is interfacial area between the organic and aqueous phases, and $K_{PPA}$ and $K_{PA}$ are the distribution coefficients for PA and PPA. In Equations (5)–(13), we used bulk concentrations in the aqueous and organic phases.

In the modeling stage, the coefficients $k_{PPA-org}$ and $k_{PA-org}$ were assumed to be similar due to the similarity between both molecules. We also assumed that these coefficients were temperature-independent. Thus, we estimated the parameter $k_{PA-org} \cdot a$.

For the estimation of $K_{PPA}$ and $K_{PA}$, we used the same approach as Wu et al. [35]. In their study, they demonstrated that these coefficients depend on the concentration of double bonds, epoxide groups, and ring-opening products:

$$K_{PA} = A.[Ep]_{org}^2 + B.[DB]_{org} + C.[RO\ products]_{org} \quad (14)$$

They also showed that the coefficient distribution of the carboxylic acid and percarboxylic acids are linked by the following relationships:

$$K_{PPA} = 0.33.K_{PA} \quad (15)$$

We estimated A, B, and C. We applied Equations (14) and (15) to express these distribution coefficients.

The volume of the dispersed organic phase, $V_{org}$, was calculated using the density calculated by Cai et al. [57,58].

### *3.3. Regression*

Regression was carried out using the software Athena Visual Studio, based on the Bayesian framework.

Ordinary differential equations from the material balances were solved using a solver named DDAPLUS [53] and were based on a modified Newton algorithm [59].

The non-linear regression was carried out using the GREGPLUS subroutine. This subroutine minimizes the objective function (OF), determines the credible intervals for each estimated parameter represented by the marginal highest posterior density (HPD), and calculates the normalized parameter covariance.

The GREGPLUS subroutine minimizes the objective function via successive quadratic programming [60]:

$$OF = (a + b + 1) \cdot ln|v| \quad (16)$$

where |υ| is the determinant of the covariance matrix of the responses, b is the number of responses, and a is the number of events in response.

Each element of this matrix is:

$$v_{ij} = \sum_{u=1}^{n} \left[C_{iu} - \hat{C}_{iu}\right] \cdot \left[C_{ju} - \hat{C}_{ju}\right] \quad (17)$$

where $C_{iu}$ is the experimental concentration, $\hat{C}_{iu}$ is the estimated value for response i and event u, $C_{ju}$ is the experimental concentration, and $\hat{C}_{ju}$ is the estimated value for response j and event u.

One should remember that the kinetic modeling for the perhydrolysis and the epoxidation is a multiresponse system, i.e., there are several observables. Van Boekel [58] stated that the Bayesian framework is more adequate than the non-linear least square approach.

It is vital to use a modified Arrhenius equation to express the temperature dependency of the rate constants [61]:

$$k_{rx}(T) = exp\left[ln\left(k_{rx}(T_{ref})\right) + \frac{E_{a_{rx}}}{R \cdot T_{ref}} \cdot \left(1 - \frac{T_{ref}}{T}\right)\right], \quad (18)$$

where $k_{rx}(T)$ is the rate constant for reaction *rx* at reaction temperature T, $E_{a_{rx}}$ is the activation energy of reaction *rx*, R is the ideal gas constant, and $T_{ref}$ is the reference temperature.

3.3.1. Kinetic Modeling of Propionic Acid Perhydrolysis

Epoxidation of vegetable oils through the Prileschajew method [17] requires the estimation of several parameters. We have developed a kinetic model only for the perhydrolysis of propionic acid, and for that we only performed experiments in the presence of propionic acid, water, hydrogen peroxide, and Amberlite IR-120 (Table 3). Table 3 shows the experimental matrix used for this modeling, and one can notice that the initial operating conditions (concentrations, temperature, catalyst loading) varied for these seven runs.

**Table 3.** Experimental matrix for the modeling of propionic acid perhydrolysis. (HP: hydrogen peroxide, PA: propionic acid, and PPA: perpropionic acid).

| Run | Dried Amberlite IR-120 (g) | T (K) | Initial [$H_2O$] (mol/L) | Initial [HP] (mol/L) | Initial [PA] (mol/L) | Initial [PPA] (mol/L) |
|---|---|---|---|---|---|---|
| 1 | 9.80 | 343.15 | 27.51 | 4.06 | 4.95 | 0.00 |
| 2 | 9.80 | 333.15 | 27.82 | 4.09 | 4.86 | 0.00 |
| 3 | 9.80 | 353.15 | 27.51 | 4.06 | 4.95 | 0.00 |
| 4 | 7.00 | 333.15 | 30.31 | 7.04 | 2.90 | 0.00 |
| 5 | 7.00 | 343.15 | 29.95 | 7.01 | 3.00 | 0.00 |
| 6 | 5.00 | 333.15 | 21.08 | 3.00 | 7.00 | 0.00 |
| 7 | 5.00 | 343.15 | 21.09 | 3.00 | 7.00 | 0.00 |

The concentrations of PA and PPA were tracked. Experiments were carried out in isothermal conditions and ideal batch reactors, thus, the material balances led to the following ODEs:

$$\frac{d[PA]_{aq}}{dt} = -R_{Perh} \quad (19)$$

$$\frac{d[PPA]_{aq}}{dt} = R_{Perh} \quad (20)$$

$$\frac{d[HP]_{aq}}{dt} = -R_{Perh} \quad (21)$$

$$\frac{d[W]_{aq}}{dt} = R_{Perh} \quad (22)$$

A van't Hoff equation was used to express the dependency of $K_{eq}$ towards the reaction temperature.

$$K_{eq}(T) = K_{eq}(T = 303.15) \cdot exp\left[\frac{-\Delta H_{Perh}}{R} \cdot \left(\frac{1}{T} - \frac{1}{303.15}\right)\right] \quad (23)$$

In this modeling, $K_{eq}(T{=}303.15)$ was fixed to 2.051 and $\Delta H_{Perh}$ to -4.17 kJ/mol, as in the reference of Leveneur et al. [55,62].

We have estimated the following kinetic constants: $ln\left(k_{Perh}(T_{ref})\right)$ and $\frac{E_{a_{Perh}}}{R \cdot T_{ref}}$, displayed in Table 4. The correlation between these two kinetic constants was found to be 0.706, lower than 0.95 [63]. Thus, both kinetic constants are not correlated.

**Table 4.** Kinetic constants and credible intervals at $T_{ref}$ = 343.15K.

| | Units | Estimates | HPD (%) |
|---|---|---|---|
| $ln\left(k_{Perh}(T_{ref})\right)$ | L/mol/g of dried cat/min | -8.57 | 0.63 |
| $\frac{E_{a_{Perh}}}{R \cdot T_{ref}}$ | - | 16.87 | 13.38 |

Figure 10 shows the fit of the model to experimental concentrations for Run 6. One can notice that the developed model fits well with the experimental concentrations.

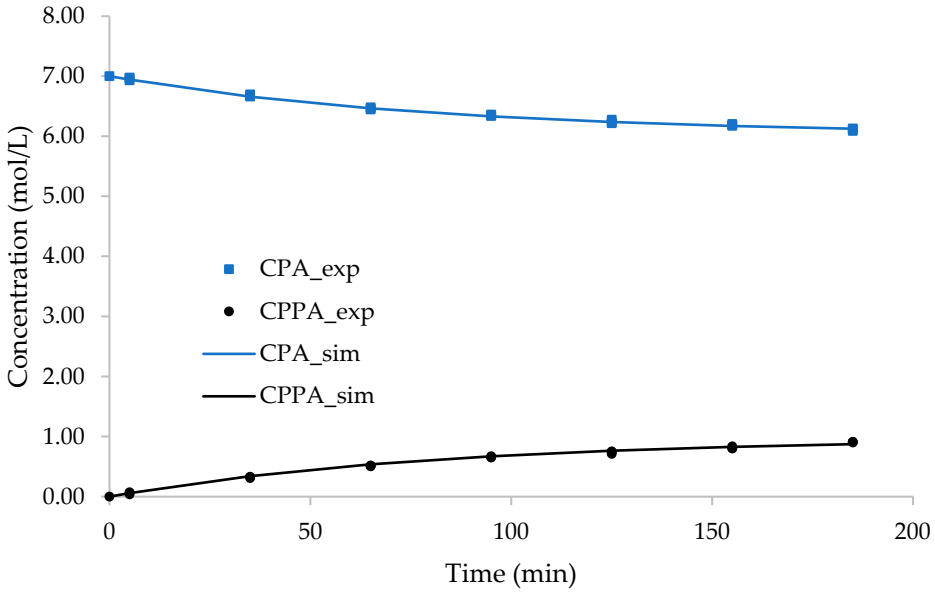


**Figure 10.** The fit of the model to experimental concentrations for Run 6. (PPA: perpropionic acid and PA: propionic acid).

Figure 11 shows the parity plots for PA and PPA, showing the excellent fit of the model.

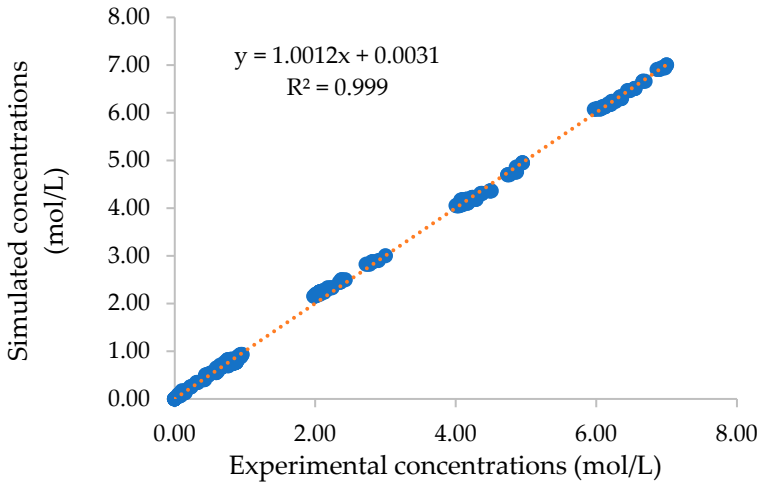


**Figure 11.** Parity plots for PA (propionic acid) and PPA (perpropionic acid) from the kinetic model of propionic acid perhydrolysis over amberlite IR-120.

### 3.3.2. Kinetic Modeling of Epoxidation

For this model, six observables ($[Ep]_{org}$, $[DB]_{org}$, $[PA]_{org}$, $[PA]_{aq}$, $[PPA]_{aq}$, and $[HP]_{aq}$) were used to estimate the kinetic constants and mass transfer parameters. The perhydrolysis kinetic and thermodynamic constants estimated in the previous section were used. Table 1 shows the experimental matrix used to develop the kinetic model for epoxidation. The ratio $m_{initial,org}/m_{initial,aq}$ was kept constant.

ODEs (5)–(13) were solved, and the following parameters were estimated: $ln\left(k_{Ep}(T_{ref})\right)$, $\frac{Ea_{Ep}}{R \cdot T_{ref}}$, $ln\left(k_{RO}(T_{ref})\right)$, $\frac{Ea_{RO}}{R \cdot T_{ref}}$, $k_{PA-org} \cdot a$, A, B and C.

Table 5 shows the values of the estimated parameters and their credible intervals. Credible intervals are generally low, indicating that the parameters are well identified. The credible interval for $k_{PA-org} \cdot a$ is large, since the temperature effect on this value was not considered.

**Table 5.** Estimated parameters and their credible intervals for the epoxidation of cottonseed oil at $T_{ref}$= 343.15 K.

| | Units | Estimates | HPD (%) |
|---|---|---|---|
| $ln\left(k_{Ep}(T_{ref})\right)$ | L/mol/min | -1.43 | 16.14 |
| $\frac{E_{a_{Ep}}}{R \cdot T_{ref}}$ | - | 12.76 | 30.59 |
| $ln\left(k_{RO}(T_{ref})\right)$ | 1/min | -8.06 | 0.81 |
| $\frac{E_{a_{RO}}}{R \cdot T_{ref}}$ | - | 13.86 | 18.58 |
| $k_{PA-org} \cdot a$ | L/min | 0.50 | >100 |
| A | $L^2/mol^2$ | 0.24 | 10.21 |
| B | L/mol | 0.92 | 6.92 |
| C | L/mol | 0.45 | 19.40 |

Table 6 shows that all estimated parameters are not correlated, meaning they were well identified.

**Table 6.** Correlation matrix of estimated parameters.

| | $ln\left(k_{Ep}(T_{ref})\right)$ | $\frac{E_{a_{Ep}}}{R \cdot T_{ref}}$ | $ln\left(k_{RO}(T_{ref})\right)$ | $\frac{E_{a_{RO}}}{R \cdot T_{ref}}$ | $k_{PA-org} \cdot a$ | A | B | C |
|---|---|---|---|---|---|---|---|---|
| $ln\left(k_{Ep}(T_{ref})\right)$ | 1 | | | | | | | |
| $\frac{E_{a_{Ep}}}{R \cdot T_{ref}}$ | 0.70 | 1 | | | | | | |
| $ln\left(k_{RO}(T_{ref})\right)$ | 0.18 | 0.07 | 1 | | | | | |
| $\frac{E_{a_{RO}}}{R \cdot T_{ref}}$ | 0.02 | 0.12 | -0.03 | 1 | | | | |
| $k_{PA-org} \cdot a$ | -0.80 | -0.41 | -0.13 | 0.01 | 1 | | | |
| A | 0.36 | 0.17 | 0.21 | -0.17 | -0.34 | 1 | | |
| B | -0.07 | -0.16 | 0.00 | -0.03 | 0.26 | -0.32 | 1 | |
| C | -0.13 | -0.04 | 0.06 | 0.11 | 0.13 | -0.65 | 0.13 | 1 |

In general, the model fits the experimental data quite well, as shown by the parity plot (Figure 12). Figure 13 displays the fit of the model to experimental data for Run 10. Figure 13 shows that the mass transfer of PA from the aqueous phase to the organic phase is very fast. The model exhibits a slight tendency to underestimate the experimental concentrations of DB and PPA, and slightly overestimates the experimental concentration of epoxide group (Ep).

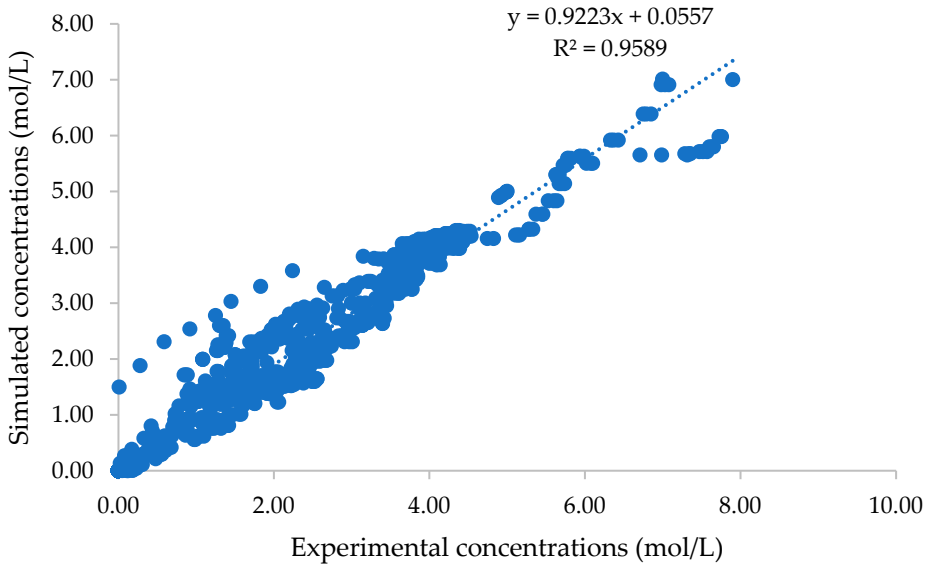


**Figure 12.** Parity plots for $[PA]_{aq}$, $[PA]_{org}$, $[PPA]_{aq}$, $[HP]_{aq}$, $[EP]_{org}$, and $[DB]_{org}$ from the kinetic model of propionic acid perhydrolysis over Amberlite IR-120. (DB: double bond, EP: epoxide, PPA: perpropionic acid, PA: propionic acid, and HP: hydrogen peroxide).

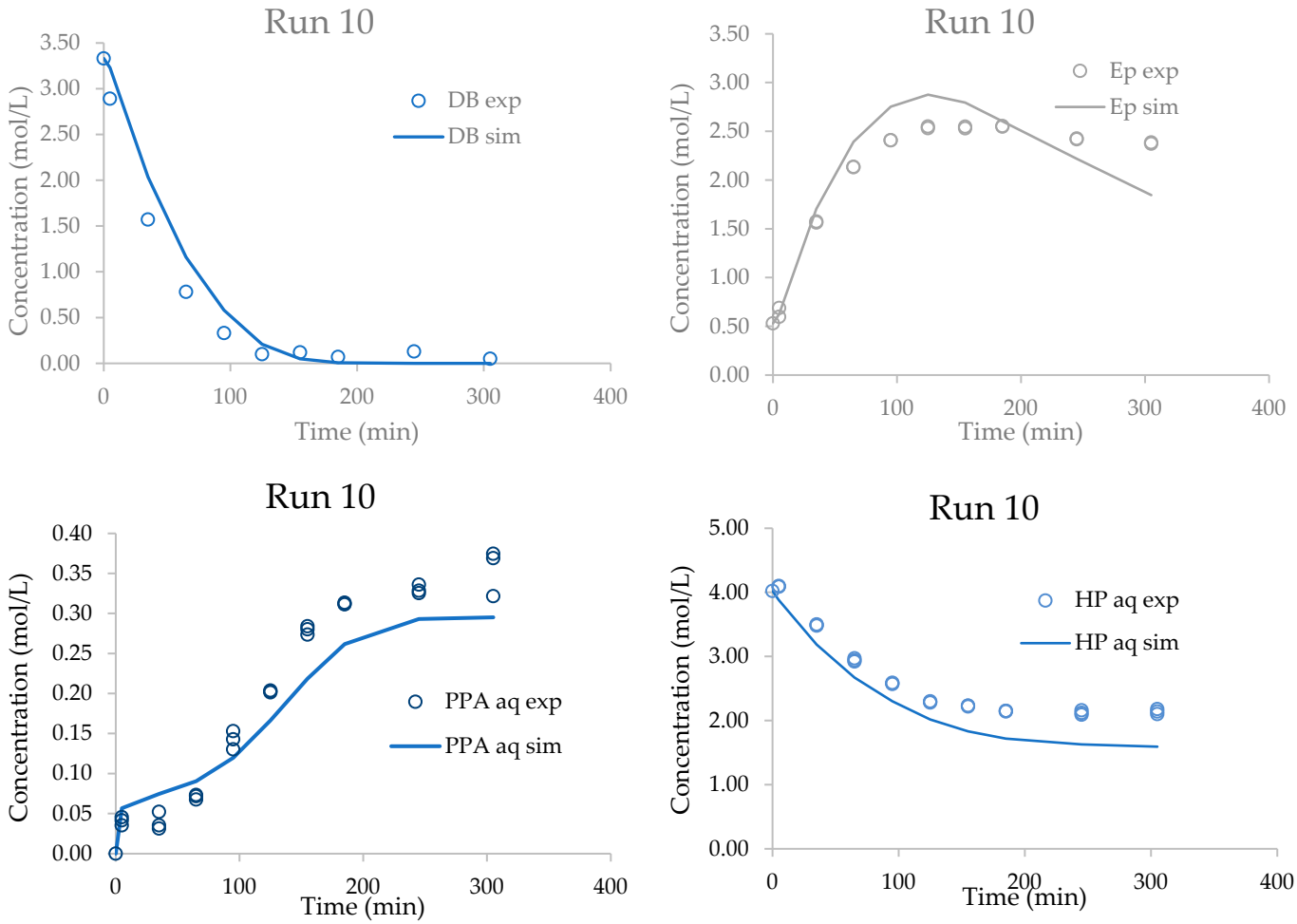

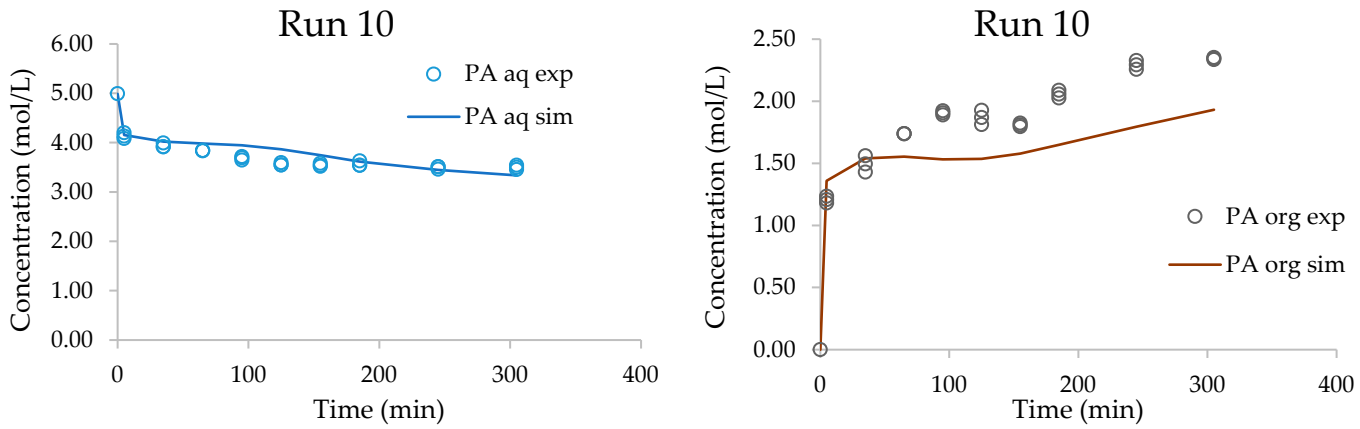


**Figure 13.** The fit of the model to Run 10. (DB: double bond, EP: epoxide, PPA: perpropionic acid, PA: propionic acid, and HP: hydrogen peroxide).

### *3.4. Validation*

A hold-out method was used to validate the model. Table 2 shows the experimental matrix used for the validation. Figure 14 represents the parity plot for the validation stage. One can notice that the model can fit the experimental concentrations for validation.

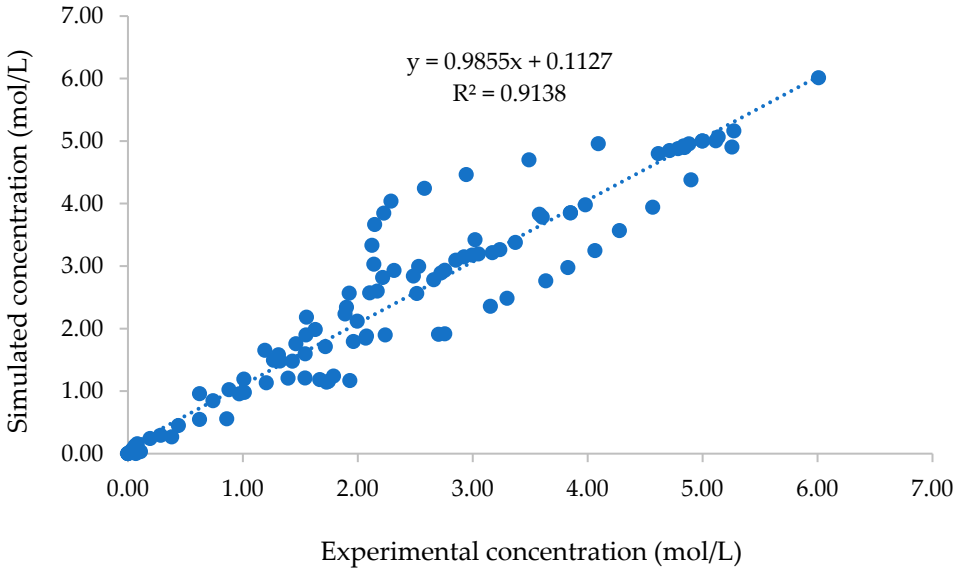


**Figure 14.** Parity plots for $[PA]_{aq}$, $[PA]_{org}$, $[PPA]_{aq}$, $[HP]_{aq}$, $[EP]_{org}$, and $[DB]_{org}$ from the kinetic model of propionic acid perhydrolysis over Amberlite IR-120 for Runs 1V and 2V. (DB: double bond, EP: epoxide, PPA: perpropionic acid, PA: propionic acid, and HP: hydrogen peroxide).

Figure 15 shows the fit of the model to the validated experimental concentrations of DB and EP for Runs 1V and 2V. For the sake of clarity, Figure 15 shows the concentrations of DB and EP. One can notice that the model slightly underestimates the experimental concentrations of EP.

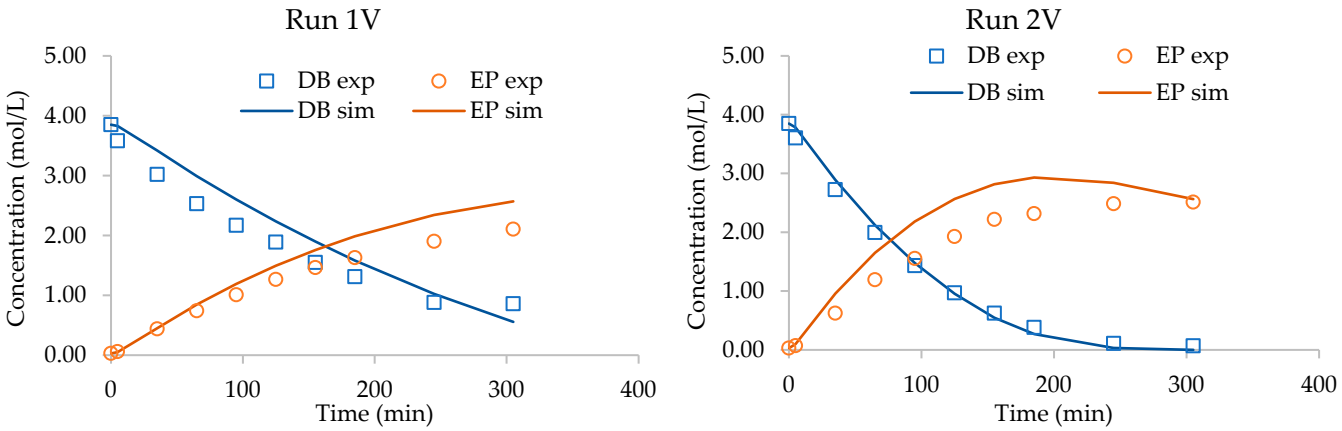


**Figure 15.** The fit of the model to Runs 1V and 2V for the validation stage. (DB: double bond and EP: epoxide).

## 4. Materials and Methods

### *4.1. Materials and Chemicals*

The following chemicals were used: refined CSO was purchased from ThermoFisher Scientific (Schwerte, Germany). Hydrogen peroxide (33 wt% in water), propionic acid (purity > 99 wt%), tetraethylammonium bromide (TEAB; 99 wt%), and perchloric acid standardized solution in acetic acid (0.1 mol/L) were obtained from VWR International (Fontenay-sous-Bois, France). Chloroform (purity > 99 wt%), iodine solution (0.1 mol/L), ferroin indicator solution, sodium thiosulfate (0.1 mol/L) solution, ammonium cerium (IV) sulfate solution (0.1 mol/L), and amberlite IR-120 were obtained from Sigma-Aldrich (Sigma-Aldrich Chemical Co., USA). 2-propanol and potassium iodide were obtained from CARLO ERBA Reagents GmbH (Milan, Cornaredo). Sodium thiosulfate solution (0.1 mol/L) and sulfuric acid (purity 95 wt%) were purchased from ThermoFisher Scientific (Schwerte, Germany).

### *4.2. Reaction*

Experiments were performed in a 300 mL glass water-jacketed reactor equipped with mechanical agitation (pitched blade turbine impeller with a diameter of 3.8 cm and four blades), a reflux condenser, and two temperature probes to measure the temperatures of the reaction mixture and outlet of the jacket. A mixture of cottonseed oil, hydrogen peroxide, distilled water, and amberlite IR-120 was added to the reactor for the epoxidation procedure. When the mixture temperature reached the desired value, a preheated propionic acid solution was added to start the reaction. During the reaction, samples were collected at different times (approximately at 0, 5, 35, 65, 95, 125, 155, 185, 245, and 305 min). After being taken from the reactor, the organic and aqueous phases were separated using a centrifuge (Rotofix 32 A, Hettich, Tuttlingen, Germany) at 6000 rpm/min for 4 min. Then, both phases were analyzed and kept in a fridge at 4 °C. At the end of the reaction, the agitation system was stopped to stratify the mixture into two phases. The same experimental approach was used for the perhydrolysis of propionic acid.

Tables 1–3 display the experimental matrix for the modeling of propionic acid perhydrolysis over amberlite IR-120 for the regression stage, the modeling of cottonseed oil epoxidation by perpropionic acid produced in situ, and the validation stage for the epoxidation model, respectively.

### *4.3. Analytical Methods*

After collecting the samples in the reaction stage and separating by centrifuging, the two phases were then analyzed using titration and spectroscopy methods to determine the concentration of double bonds, epoxidized groups, and carboxylic acid in the organic

phase. The concentration of acids and hydrogen peroxide in the aqueous phase was measured using titration. NMR, FTIR, and GPC were used to characterize the organic phase further and get inside for the polymerization and ring-opening reactions.

#### 4.3.1. NMR

$^1$H NMR analysis was performed on a Bruker 300 Fourier Transform spectrometer (Bruker Corporation, Billerica, United States) at 300 MHz in $CDCl_3$ solutions containing tetramethylsilane (TMS) as an internal standard.

#### 4.3.2. FTIR

FTIR spectra were acquired with a Perkin-Elmer Spectrum 2000 FTIR (Perkin-Elmer, Waltham, United States) equipped with a diamond ATR device (attenuated total reflection). Spectra were recorded from 10 scans in the 650 to 4000 $cm^{-1}$ range.

#### 4.3.3. GPC

The average molecular weights of polymers (Mn and Mw) and dispersity (Đ = Mw/Mn) were assessed through size exclusion chromatography (sEc). Polymers were dissolved in dichloromethane, filtered (0.45 μm), and analyzed at 25°C using a Varian PL-GPC50 system (Agilent Technologies, Santa Clara, United States) equipped with two mixed packed columns (PL gel mixed type C). Dichloromethane was used as the mobile phase and PMMA standards (from 875 to 62,000 g $mol^{-1}$) were used for calibration.

#### 4.3.4. Double Bond Content

The concentration of the double bonds was measured using the iodine value, which was determined by the Wijs method [64]. Briefly, 0.20 g of oil sample or organic phase was dissolved in 20 mL of chloroform. Then, 25 mL of Wijs solution (0.1 mol/L iodine monochloride in glacial acetic acid) was added and kept in a dark place for 1 h. After a one-hour reaction, 20 mL of 10% potassium iodide solution was added to stop the reaction. After adding 100 mL water, the mixture solution was titrated using sodium thiosulphate solution (0.1 mol/L) with an automatic titrator (916 Ti-Touch, Methrohm, Herisau, Switzerland).

#### 4.3.5. Epoxide Content

The concentration of epoxide groups was determined by the method of Jay [65]. Briefly, 0.10 g of oil sample or organic phase was dissolved in 10 mL of chloroform. After adding 10 mL of 20% TEAB solution in acetic acid, the mixture solution was titrated using standard perchloric acid in acetic acid solution (0.1 mol/L) with an automatic titrator (916 Ti-Touch, Methrohm Herisau, Switzerland)).

#### 4.3.6. Hydrogen Peroxide Content

The concentration of hydrogen peroxide was determined by the method of Greenspan and Mackellar [66]. Briefly, 0.20 g of aqueous phase was dissolved in 50 mL of 10% sulfuric acid in water solution. Then, three drops of Ferroin indicator solution were added and titrated using standard ammonium cerium sulfate solution (0.1 mol/L) until the color of the mixture solution reached a light blue endpoint.

#### 4.3.7. Concentration of Acid

The concentration of acid was determined by the titration method [30]. For the concentration of acid in the aqueous phase, a 0.30 g sample was dissolved in 50 mL distilled water and titrated using sodium hydroxide solution (0.1 mol/L) with an automatic titrator (916 Ti-Touch). For the organic phase, a 0.50 g sample was dissolved in 50 mL 2-propanol and titrated in the same way as above.

## 5. Conclusions

The production of epoxidized vegetable oils by the Prileschajew method is still the most used because it circumvents the low hydrogen peroxide solubility by producing a percarboxylic acid in situ. Nevertheless, this method has two drawbacks: thermal instability of the produced percarboxylic acid and the oxirane ring-opening side reaction by protons. A trade-off between the percarboxylic acid thermal instability and its reactivity was found by using perpropionic acid. The use of a solid acid catalyst accelerates the production of percarboxylic acid, and lowers the ring-opening side reaction because the accessibility of the acid sites to the oxirane groups due to steric hindrance is reduced. For this reason, amberlite IR-120 was used in this study. The kinetics of cottonseed oil epoxidation by perpropionic acid produced in situ was studied in an isothermal batch reactor.

A biphasic kinetic model taking into account the mass transfer of propionic acid and perpropionic acid from the aqueous continuous phase to the organic dispersed phase was developed and assessed. A Bayesian approach was used to estimate and evaluate kinetic constants and mass transfer coefficients. We developed the following kinetic modeling strategy to decrease the number of parameters to estimate: first, only model the kinetics of propionic acid perhydrolysis, which produces perpropionic acid; second, model the kinetics of the epoxidation of cottonseed oil by perpropionic acid produced in situ. A hold-out method was used to validate the epoxidation kinetic model. An in-depth analysis (NMR, GPC, FTIR, titration) was carried out to understand the ring-opening reaction, and we found that water and diol were responsible for this side reaction.

The cottonseed oil epoxidation model was found to be reliable for the following initial operating conditions: dried catalyst amount from 2 to 15 g, reaction temperature from 323.15 to 353.15 K, double bond initial concentrations from 3.33 to 3.85 mol/L, initial propionic acid concentration in the aqueous phase from 3 to 7 mol/L, and initial hydrogen peroxide concentrations from 3 to 7.01 mol/L.

A continuation of this work could be the comparison with other carboxylic acids, and an investigation on the catalyst interaction between the aqueous and organic phases.

**Author Contributions:** Conceptualization, Y.M., X.C., N.,K and S.L.; methodology, Y.M., X.C., N.,K and S.L.; software, S.L.; validation, Y.M.; writing—original draft preparation, Y.M., X.C., N.,K and S.L.; writing—review and editing, Y.M., X.C., N.,K and S.L.; supervision, N.K. and S.L.; funding acquisition, S.L. All authors have read and agreed to the published version of the manuscript.

**Funding:** This article is part of the ARBRE project. ARBRE is co-funded by the European Union through the European Regional Development Fund (ERDF) and by Normandy Region, via the support of "pôle CTM (Continuum Terre-Mer) and EP2M (Energies, Propulsion, Matière, Matériaux) de Normandie université". The China Scholarship Council: Cooperation Program with the UTs and INSAs (France) is thanked by the authors.

**Conflicts of Interest:** The authors declare no conflicts of interest.

## References

1. Gebremariam, S.N.; Marchetti, J.M. Biodiesel production technologies: Review. *AIMS Energy* **2017**, *5*, 425–457.
2. Mittal, V.; Talapatra, K.N.; Ghosh, U.K. A comprehensive review on biodiesel production from microalgae through nanocatalytic transesterification process: Lifecycle assessment and methodologies. *Int. Nano Lett.* **2022**, *12*, 351–378. https://doi.org/10.1007/s40089-022-00372-2.
3. Leung, D.Y.C.; Wu, X.; Leung, M.K.H. A review on biodiesel production using catalyzed transesterification. *Appl. Energy* **2010**, *87*, 1083–1095.
4. Salaheldeen, M.; Mariod, A.A.; Aroua, M.K.; Rahman, S.M.A.; Soudagar, M.E.M.; Fattah, I.M.R. Current state and perspectives on transesterification of triglycerides for biodiesel production. *Catalysts* **2021**, *11*, 1121.
5. Alsultan, A.G.; Asikin-Mijan, N.; Ibrahim, Z.; Yunus, R.; Razali, S.Z.; Mansir, N.; Islam, A.; Seenivasagam, S.; Taufiq-Yap, Y.H. A short review on catalyst, feedstock, modernised process, current state and challenges on biodiesel production. *Catalysts* **2021**, *11*, 1261.
6. Lligadas, G.; Ronda, J.C.; Galià, M.; Cádiz, V. Renewable polymeric materials from vegetable oils: A perspective. *Mater. Today* **2013**, *16*, 337–343.

7. Adekunle, K.F. A Review of Vegetable Oil-Based Polymers: Synthesis and Applications. *Open, J. Polym. Chem.* **2015**, *5*, 34–40. https://doi.org/10.4236/ojpchem.2015.53004.
8. Maisonneuve, L.; Lamarzelle, O.; Rix, E.; Grau, E.; Cramail, H. Isocyanate-Free Routes to Polyurethanes and Poly(hydroxy Urethane)s. *Chem. Rev.* **2015**, *115*, 12407–12439.
9. Lligadas, G. Renewable polyols for polyurethane synthesis via thiol-ene/yne couplings of plant oils. *Macromol. Chem. Phys.* **2013**, *214*, 415–422. https://doi.org/10.1002/macp.201200582.
10. Guzmán Agudelo, A.F.; Pérez-Sena, W.Y.; Kebir, N.; Salmi, T.; Ríos, L.A.; Leveneur, S. Influence of steric effects on the kinetics of cyclic-carbonate vegetable oils aminolysis. *Chem. Eng. Sci.* **2020**, *228*, 115954. https://doi.org/10.1016/j.ces.2020.115954.
11. Pérez-Sena, W.Y.; Cai, X.; Kebir, N.; Vernières-Hassimi, L.; Serra, C.; Salmi, T.; Leveneur, S. Aminolysis of cyclic-carbonate vegetable oils as a non-isocyanate route for the synthesis of polyurethane: A kinetic and thermal study. *Chem. Eng. J.* **2018**, *346*, 271–280. https://doi.org/10.1016/j.cej.2018.04.028.
12. Meng, Y.; Taddeo, F.; Aguilera, A.F.; Cai, X.; Russo, V.; Tolvanen, P.; Leveneur, S. The lord of the chemical rings: Catalytic synthesis of important industrial epoxide compounds. *Catalysts* **2021**, *11*, 765.
13. Scotti, N.; Ravasio, N.; Psaro, R.; Evangelisti, C.; Dworakowska, S.; Bogdal, D.; Zaccheria, F. Copper mediated epoxidation of high oleic natural oils with a cumene-O2 system. *Catal. Commun.* **2015**, *64*, 80–85. https://doi.org/10.1016/j.catcom.2015.02.008.
14. Perez-Sena, W.Y.; Wärnå, J.; Eränen, K.; Tolvanen, P.; Estel, L.; Leveneur, S.; Salmi, T. Use of semibatch reactor technology for the investigation of reaction mechanism and kinetics: Heterogeneously catalyzed epoxidation of fatty acid esters. *Chem. Eng. Sci.* **2021**, *230*, 116206. https://doi.org/10.1016/j.ces.2020.116206.
15. Wisniak, J.; Cancino, A.; Vega, J.C. Epoxidation of Anchovy Oils. A Study of Variables. *I&EC Prod. Res. Dev.* **1964**, *3*, 306–311. https://doi.org/10.1021/i360012a012.
16. Wisniak, J.; Navarrete, E. Epoxidation Of Fish Oil Kinetic and Optimization Model. *Ind. Eng. Chem. Prod. Res. Dev.* **1970**, *9*, 33–41. https://doi.org/10.1021/i360033a006.
17. Prileschajew, N. Oxydation ungesättigter Verbindungen mittels organischer Superoxyde. *Berichte der Dtsch. Chem. Gesellschaft* **1909**, *42*, 4811–4815. https://doi.org/10.1002/cber.190904204100.
18. Wai, P.T.; Jiang, P.; Shen, Y.; Zhang, P.; Gu, Q.; Leng, Y. Catalytic developments in the epoxidation of vegetable oils and the analysis methods of epoxidized products. *RSC Adv.* **2019**, *9*, 38119–38136.
19. Sienkiewicz, A.M.; Czub, P. The unique activity of catalyst in the epoxidation of soybean oil and following reaction of epoxidized product with bisphenol A. *Ind. Crops Prod.* **2016**, *83*, 755–773. https://doi.org/10.1016/j.indcrop.2015.11.071.
20. Chen, J.; De Liedekerke Beaufort, M.; Gyurik, L.; Dorresteijn, J.; Otte, M.; Klein Gebbink, R.J.M. Highly efficient epoxidation of vegetable oils catalyzed by a manganese complex with hydrogen peroxide and acetic acid. *Green Chem.* **2019**, *21*, 2436–2447. https://doi.org/10.1039/c8gc03857k.
21. Aguilera, A.F.; Tolvanen, P.; Eränen, K.; Wärnå, J.; Leveneur, S.; Marchant, T.; Salmi, T. Kinetic modelling of Prileschajew epoxidation of oleic acid under conventional heating and microwave irradiation. *Chem. Eng. Sci.* **2019**, *199*, 426–438. https://doi.org/10.1016/j.ces.2019.01.035.
22. Almasi, S.; Ghobadian, B.; Najafi, G.; Dehghani Soufi, M. A novel approach for bio-lubricant production from rapeseed oil-based biodiesel using ultrasound irradiation: Multi-objective optimization. *Sustain. Energy Technol. Assess.* **2021**, *43*, 100960. https://doi.org/10.1016/j.seta.2020.100960.
23. Zhang, M.; Cheng, Q.; Chen, T.; Wei, X.; Meng, L. Development and characterisation research on SnO2-Al2O3-NiO/SO42− catalysed epoxidation of soybean oil under hydraulic cavitation. *Appl. Organomet. Chem.* **2022**, *36*, e6617. https://doi.org/10.1002/aoc.6617.
24. Maia, D.L.H.; Fernandes, F.A.N. Influence of carboxylic acid in the production of epoxidized soybean oil by conventional and ultrasound-assisted methods. *Biomass Convers. Biorefinery* **2020**, *12*, 5861–5868. https://doi.org/10.1007/s13399-020-01130-0.
25. Leveneur, S.; Ledoux, A.; Estel, L.; Taouk, B.; Salmi, T. Epoxidation of vegetable oils under microwave irradiation. *Chem. Eng. Res. Des.* **2014**, *92*, 1495–1502. https://doi.org/10.1016/j.cherd.2014.04.010.
26. Leveneur, S. Thermal Safety Assessment through the Concept of Structure-Reactivity: Application to Vegetable Oil Valorization. *Org. Process Res. Dev.* **2017**, *21*, 543–550. https://doi.org/10.1021/acs.oprd.6b00405.
27. Casson Moreno, V.; Russo, V.; Tesser, R.; Di Serio, M.; Salzano, E. Thermal risk in semi-batch reactors: The epoxidation of soybean oil. *Process Saf. Environ. Prot.* **2017**, *109*, 529–537. https://doi.org/10.1016/j.psep.2017.05.001.
28. Rakotondramaro, H.; Wärnå, J.; Estel, L.; Salmi, T.; Leveneur, S. Cooling and stirring failure for semi-batch reactor: Application to exothermic reactions in multiphase reactor. *J. Loss Prev. Process Ind.* **2016**, *43*, 147–157. https://doi.org/10.1016/j.jlp.2016.05.011.
29. Leveneur, S.; Pinchard, M.; Rimbault, A.; Safdari Shadloo, M.; Meyer, T. Parameters affecting thermal risk through a kinetic model under adiabatic condition: Application to liquid-liquid reaction system. *Thermochim. Acta* **2018**, *666*, 10–17. https://doi.org/10.1016/j.tca.2018.05.024.
30. Cai, X.; Zheng, J.L.; Aguilera, A.F.; Vernières-Hassimi, L.; Tolvanen, P.; Salmi, T.; Leveneur, S. Influence of ring-opening reactions on the kinetics of cottonseed oil epoxidation. *Int. J. Chem. Kinet.* **2018**, *50*, 726–741. https://doi.org/10.1002/kin.21208.
31. Jalil, M.J.; Azmi, I.S.; Yamin, A.F.M.; Yeop, M.Z.; Hadi, A. Catalytic Epoxidation of Oleic Acid and Subsequent Ring-Opening by In Situ Hydrolysis for Production Dihydroxystearic Acid. *J. Polym. Environ.* **2022**, 1–11. https://doi.org/10.1007/s10924-022-02736-3.
32. Azmi, I.S.; Ozir, T.A.Z.T.; Rasib, I.M.; Nurherdiana, S.D.; Jalil, M.J. Synergistic epoxidation of palm oleic acid using a hybrid oxygen carrier solution. *Biomass Convers. Biorefinery* **2022**, 1–8. https://doi.org/10.1007/s13399-022-03325-z.

33. Leveneur, S.; Wärnå, J.; Salmi, T.; Murzin, D.Y. Catalytic synthesis and decomposition of peroxycarboxylic acids—Green catalytic synthesis of green compounds. *Trends Chem. Eng.* **2010**, *13*, 17–52. https://doi.org/10.1016/S0958-2118(05)70503-6.
34. Santacesaria, E.; Tesser, R.; Di Serio, M.; Turco, R.; Russo, V.; Verde, D. A biphasic model describing soybean oil epoxidation with H2O2 in a fed-batch reactor. *Chem. Eng. J.* **2011**, *173*, 198–209. https://doi.org/10.1016/j.cej.2011.05.018.
35. Wu, Z.; Nie, Y.; Chen, W.; Wu, L.; Chen, P.; Lu, M.; Yu, F.; Ji, J. Mass transfer and reaction kinetics of soybean oil epoxidation in a formic acid-autocatalyzed reaction system. *Can. J. Chem. Eng.* **2016**, *94*, 1576–1582. https://doi.org/10.1002/cjce.22526.
36. Salmi, T.; Russo, V.; Aguilera, A.F.; Tolvanen, P.; Wärnå, J.; Di Serio, M.; Tesser, R.; Cogliano, T.; Leveneur, S.; Eränen, K. A new perspective on vegetable oil epoxidation modeling: Reaction and mass transfer in a liquid–liquid–solid system. *AIChE J.* **2022**, *68*, e17626. https://doi.org/10.1002/aic.17626.
37. Zheng, J.L.; Wärnå, J.; Salmi, T.; Burel, F.; Taouk, B.; Leveneur, S. Kinetic modeling strategy for an exothermic multiphase reactor system: Application to vegetable oils epoxidation using Prileschajew method. *AIChE J.* **2016**, *62*, 726–741. https://doi.org/10.1002/aic.15037.
38. Janković, M.R.; Govedarica, O.M.; Sinadinović-Fišer, S.V. The epoxidation of linseed oil with in situ formed peracetic acid: A model with included influence of the oil fatty acid composition. *Ind. Crops Prod.* **2020**, *143*, 111881. https://doi.org/10.1016/j.indcrop.2019.111881.
39. Janković, M.; Sinadinović-Fišer, S.; Govedarica, O.; Pavličević, J.; Budinski-Simendić, J. Kinetika epoksidovanja sojinog ulja persirćetnom kiselinom formiranom in situ u prisustvu jonoizmenjivačke smole: Pseudo-homogeni model. *Chem. Ind. Chem. Eng. Q.* **2017**, *23*, 97–111. https://doi.org/10.2298/CICEQ150702014J.
40. Leveneur, S.; Zheng, J.; Taouk, B.; Burel, F.; Wärnå, J.; Salmi, T. Interaction of thermal and kinetic parameters for a liquid-liquid reaction system: Application to vegetable oils epoxidation by peroxycarboxylic acid. *J. Taiwan Inst. Chem. Eng.* **2014**, *45*, 1449–1458. https://doi.org/10.1016/j.jtice.2014.01.015.
41. Campanella, A.; Fontanini, C.; Baltanás, M.A. High yield epoxidation of fatty acid methyl esters with performic acid generated in situ. *Chem. Eng. J.* **2008**, *144*, 466–475. https://doi.org/10.1016/j.cej.2008.07.016.
42. Mungroo, R.; Goud, V.V.; Pradhan, N.C.; Dalai, A.K. Modification of epoxidised canola oil. *Asia-Pacific, J. Chem. Eng.* **2011**, *6*, 14–22.
43. Dinda, S.; Patwardhan, A.V.; Goud, V.V.; Pradhan, N.C. Epoxidation of cottonseed oil by aqueous hydrogen peroxide catalysed by liquid inorganic acids. *Bioresour. Technol.* **2008**, *99*, 3737–3744. https://doi.org/10.1016/j.biortech.2007.07.015.
44. Coud, V.V.; Pradhan, N.C.; Patwardhan, A.V. Epoxidation of karanja (Pongamia glabra) oil by H2O2. *JAOCS J. Am. Oil Chem. Soc.* **2006**, *83*, 635–640. https://doi.org/10.1007/s11746-006-1250-7.
45. Goud, V.V.; Patwardhan, A.V.; Pradhan, N.C. Studies on the epoxidation of mahua oil (*Madhumica indica*) by hydrogen peroxide. *Bioresour. Technol.* **2006**, *97*, 1365–1371. https://doi.org/10.1016/j.biortech.2005.07.004.
46. Okieimen, F.E.; Bakare, O.I.; Okieimen, C.O. Studies on the epoxidation of rubber seed oil. *Ind. Crops Prod.* **2002**, *15*, 139–144. https://doi.org/10.1016/S0926-6690(01)00104-2.
47. Abraham, M.E.; Benenati, R.F. Kinetics and mechanism of the epoxidation of unsaturated fatty acids. *AIChE J.* **1972**, *18*, 807–811. https://doi.org/10.1002/aic.690180424.
48. Leveneur, S.; Salmi, T.; Musakka, N.; WärnÅ, J. Kinetic study of decomposition of peroxypropionic acid in liquid phase through direct analysis of decomposition products in gas phase. *Chem. Eng. Sci.* **2007**, *62*, 5007–5012. https://doi.org/10.1016/j.ces.2006.12.040.
49. de Haro, J.C.; Izarra, I.; Rodríguez, J.F.; Pérez, Á.; Carmona, M. Modelling the epoxidation reaction of grape seed oil by peracetic acid. *J. Clean. Prod.* **2016**, *138*, 70–76. https://doi.org/10.1016/j.jclepro.2016.05.015.
50. Musante, R.L.; Grau, R.J.; Baltanás, M.A. Kinetic of liquid-phase reactions catalyzed by acidic resins: The formation of peracetic acid for vegetable oil epoxidation. *Appl. Catal. A Gen.* **2000**, *197*, 165–173. https://doi.org/10.1016/S0926-860X(99)00547-5.
51. Hasdemir, D.; Hoefsloot, H.C.J.; Smilde, A.K. Validation and selection of ODE based systems biology models: How to arrive at more reliable decisions. *BMC Syst. Biol.* **2015**, *9*, 32. https://doi.org/10.1186/s12918-015-0180-0.
52. Ozbuyukkaya, G.; Parker, R.S.; Veser, G. Determining robust reaction kinetics from limited data. *AIChE J.* **2022**, *68*, e17538. https://doi.org/10.1002/AIC.17538.
53. Stewart, W.E.; Caracotsios, M. *Computer-Aided Modeling of Reactive Systems*; John Wiley & Sons: Hoboken, Untied States, 2007; ISBN 9780470274958.
54. Leveneur, S.; De Araujo Filho, C.A.; Estel, L.; Salmi, T. Modeling of a liquid-liquid-solid heterogeneous reaction system: Model system and peroxyvaleric acid. *Ind. Eng. Chem. Res.* **2012**, *51*, 189–201. https://doi.org/10.1021/ie2017064.
55. Leveneur, S.; Wärnå, J.; Salmi, T.; Murzin, D.Y.; Estel, L. Interaction of intrinsic kinetics and internal mass transfer in porous ion-exchange catalysts: Green synthesis of peroxycarboxylic acids. *Chem. Eng. Sci.* **2009**, *64*, 4101–4114. https://doi.org/10.1016/j.ces.2009.05.055.
56. Leveneur, S.; Thönes, M.; Hébert, J.P.; Taouk, B.; Salmi, T. From kinetic study to thermal safety assessment: Application to peroxyformic acid synthesis. *Ind. Eng. Chem. Res.* **2012**, *51*, 13999–14007. https://doi.org/10.1021/ie3017847.
57. Cai, X.; Ait Aissa, K.; Estel, L.; Leveneur, S. Investigation of the Physicochemical Properties for Vegetable Oils and Their Epoxidized and Carbonated Derivatives. *J. Chem. Eng. Data* **2018**, *63*, 1524–1533. https://doi.org/10.1021/acs.jced.7b01075.
58. Cai, X.; Matos, M.; Leveneur, S. Structure–Reactivity: Comparison between the Carbonation of Epoxidized Vegetable Oils and the Corresponding Epoxidized Fatty Acid Methyl Ester. *Ind. Eng. Chem. Res.* **2019**, *58*, 1548–1560. https://doi.org/10.1021/acs.iecr.8b05510.

59. Caracotsios, M.; Stewart, W.E. Sensitivity analysis of initial value problems with mixed odes and algebraic equations. *Comput. Chem. Eng.* **1985**, *9*, 359–365. https://doi.org/10.1016/0098-1354(85)85014-6.
60. Stewart, W.E.; Caracotsios, M.; Sørensen, J.P. Parameter estimation from multiresponse data. *AIChE J.* **1992**, *38*, 641–650. https://doi.org/10.1002/aic.690380502.
61. Buzzi-Ferraris, G. Planning of experiments and kinetic analysis. *Catal. Today* **1999**, *52*, 125–132. https://doi.org/10.1016/S0920-5861(99)00070-X.
62. Leveneur, S.; Salmi, T.; Murzin, D.Y.; Estel, L.; Wärnå, J.; Musakka, N. Kinetic study and modeling of peroxypropionic acid synthesis from propionic acid and hydrogen peroxide using homogeneous catalysts. *Ind. Eng. Chem. Res.* **2008**, *47*, 656–664. https://doi.org/10.1021/ie070670e.
63. Toch, K.; Thybaut, J.W.; Marin, G.B. A systematic methodology for kinetic modeling of chemical reactions applied to n-hexane hydroisomerization. *AIChE J.* **2015**, *61*, 880–892. https://doi.org/10.1002/aic.14680.
64. Paquot, C. *2.504. Determination of thep-Anisidine Value (p-A.V.)*; Elsevier Science: Amsterdam, The Netherlands, 1979; ISBN 9781483280820.
65. Maerker, G. Determination of oxirane content of derivatives of fats. *J. Am. Oil Chem. Soc.* **1965**, *42*, 329–332. https://doi.org/10.1007/BF02540140.
66. Greenspan, F.P.; MacKellah, D.G. Analysis of Aliphatic Per Acids. *Anal. Chem.* **1948**, *20*, 1061–1063. https://doi.org/10.1021/ac60023a020.